Università di Pisa

Simulation of one-dimensional subband transport in ultra-short silicon nanowire transistors

Gianluca Fiori
Dipartimento di Ingegneria dell'Informazione: Elettronica, Informatica, Telecomunicazioni, Università di Pisa
Giuseppe Iannaccone
Dipartimento di Ingegneria dell'Informazione: Elettronica, Informatica, Telecomunicazioni, Università di Pisa

G. Fiori, G. Iannaccone, Simulation of one-dimensional subband transport in ultra-short silicon nanowire transistors, 6th International Conference on the Ultimate Integration of Silicon, pp. 163-166, Bologna 2005.

Simulation of one dimensional subband transport in ultra-short silicon nanowire transistors

Gianluca Fiori[1,*] and Giuseppe Iannaccone[1,2,**]
[1] *Dipartimento di Ingegneria dell'Informazione, University of Pisa 56100 Pisa, Italy*
[2] *IEIIT-CNR, Via Caruso, I-56122 Pisa, Italy*
email: [*]g.fiori@iet.unipi.it,
[**]g.iannaccone@iet.unipi.it

Abstract

In this paper we present three-dimensional (3D) simulations of nanowire transistors (SNWTs), based on the self-consistent solution of the Poisson and Schrödinger equations, in which two dimensional confinement and one-dimensional (1D) transport of electrons in the channel have been considered. In particular, the continuity equation has been solved in 1D subbands for both the semiclassical and quantum ballistic regime, and in the drift-diffusion regime, in order to consider both limiting cases.

I. INTRODUCTION

Silicon Nano Wire Transistors represent a promising alternative architecture to the conventional planar technology for devices at the end of the ITRS roadmap [1], because of the improved electrostatic control of the channel via the gate voltage and the consequent suppression of short channel effects [2–5]. Since electrostatic play an important role in these devices, simulations can represent a valid tool in order to understand device behavior and to give design guidelines. Three-dimensional drift-diffusion simulations have been performed in Refs. [2, 3] to study the optimum configuration that reduces short channel effects, and in [6–8], where quantum corrections to the electron density have been considered. In [9] instead, a simulation study of ballistic SNWTs with different cross sections, has shown advantages with respect to Double Gate MOSFETs, as far as downscaling is concerned.

Here we focus on some important aspects of the electrical properties of SNWTs that are still open. Indeed, as demonstrated in [10], silicon MOSFETs with effective channel length smaller than 50 nm will not be fully ballistic, so it is reasonable to assume that even for SNWTs scattering events can occur and a fully ballistic assumption can be considered as a limiting case. Transport in SNWT is then likely to be in an intermediate regime between ballistic and drift-diffusion, and its simulation would require the detailed knowledge of the scattering rates of electrons in the 1D subbands. Relevant information can be obtained by considering the two limiting cases (ballistic and drift-diffusion), assuming that a partially ballistic transistor would have an intermediate behavior. Another important aspect of interest is source-to-drain tunneling, that is expected to have a significant impact on the shortest devices.

Here, we investigate the electrical properties of SNWTs using an in-house developed 3D code based on density functional theory, in which Poisson, Schrödinger, and current continuity equations are solved self-consistently in the 3D domain, to understand what are the scaling prospectives of such devices, the achievable performance, and the relevance of source-to-drain tunneling. The Schrödinger equation is decoupled adiabatically in a series of 2D equations on each transversal slice and 1D equation along the transport direction.

In particular, we have considered a device structure with rectangular cross section (5 nm $\times$ 5 nm), in which fully ballistic and drift-diffusion transport in 1D subbands has been considered. As a consequence, we have been able to define an upper and a lower limit for the SNWT performance, deriving significant quantities such as the DIBL and the subthreshold swing as a function of channel length.

II. PHYSICAL MODELS AND NUMERICAL METHOD

The three-dimensional Poisson/Schrödinger equation has been solved self-consistently with Density Function Theory (DFT), in the local density approximation [11], by means of the Newton-Raphson algorithm with the predictor/corrector scheme similar to that proposed in [12]. In particular, the Schrödinger equation is solved at the beginning of each NR cycle, then, the eigenfunctions are kept constant until the NR cycle converges (i.e. the correction on the potential is smaller than a predetermined value), while the eigenvalues are adjusted by a quantity equal to $\phi - \tilde{\phi}$, where ϕ is the potential computed at each NR cycle, while $\tilde{\phi}$ is the potential used to computed the Schrödinger equation.

Since in the considered devices, the confinement is strong in the plane perpendicular to the current direction, we have decoupled the Schrödinger equation in a two dimensional equation in the plane of confinement, while continuous states have been considered in the direction of propagation [13].

Energy levels split in well separated 1D subbands, that we assume to be uncoupled.

In particular, in order to define an upper limit for the device performance, we have solved the continuity equation in each subband in the fully ballistic approximation, both in the semiclassical and in the quantum case.

The source-to-drain current (I_{DS_i}) in the generic i-*th* subband E_i reads,

$$I_{DS_i} = \frac{qK_BT}{\pi\hbar}\int_0^\infty dE\tau_i(E)\left[f_S(E) - f_D(E)\right] \qquad (1)$$

where K_BT is the thermal energy, $\hbar$ is Plank's constant, and f_S and f_D are the Fermi-Dirac functions with the Fermi level of the source and the drain, respectively. The transmission coefficient $\tau_i(E)$, in the semiclassical case, is zero for energy below the maximum of E_i, and equal to one otherwise [14], while, in the quantum case, it is computed by means of the transmission matrix formalism.

The lower limit of device performance is represented by the drift-diffusion transport, addressed with the Scharfetter and Gummel scheme [15].

In particular, the density current for electrons in the $i-th$ subband (J_{n_i}) reads

$$J_{n_i} = q\mu_n n_{1D_i}\frac{\partial E_i}{\partial x} + qD_n\frac{\partial n_{1D_i}}{\partial x} \qquad (2)$$

where n_{1D_i} is the linear electron density, and μ_n and D_n are the mobility and the diffusion coefficients for electrons, respectively.

For what concerns the mobility, velocity saturation has been taken into account by means of the Caughey-Thomas model [16],

$$\mu_n = \frac{\mu_0}{\left[1 + \left(\frac{\mu_0\mathcal{E}_l}{v_{sat}}\right)^\gamma\right]^{\frac{1}{\gamma}}} \qquad (3)$$

where $\mathcal{E}_l$ is the longitudinal field, v_{sat} is the velocity saturation ($v_{sat} = 1.1\times10^7$ cm/s), γ is a constant fitting parameter ($\gamma = 2$ is a common value for electrons at room temperature), while μ_0 has been computed by means of the Mathienssen's rule combining lattice, and impurities scattering described by the unified mobility model proposed by Klassen [17].

Once computed n_{1D_i}, the three-dimensional electron density (n) reads

$$n = \sum_i |\psi_i|^2 n_{1D_i} \qquad (4)$$

where $|\psi_i|$ are the eigenfunctions associated with the $i-th$ subband.

From a numerical point of view, we note that eq. (4) does not obey, as it is, to the the predictor/corrector scheme, since it does not depend explicitly to the potential ϕ at each NR cycle. Indeed we have encountered convergence problem, that on the other hand can

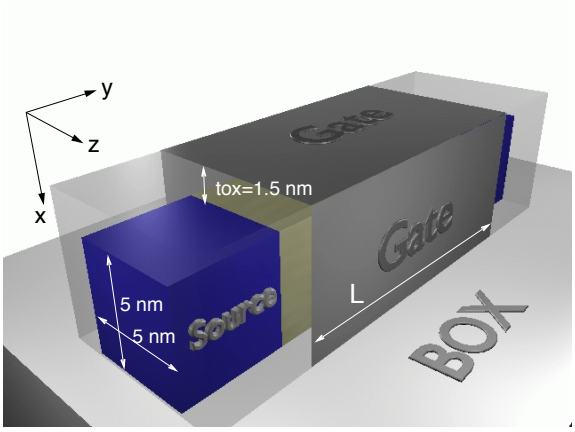

FIG. 1: Three-dimensional structure of the simulated Silicon Nanowire Transistor.

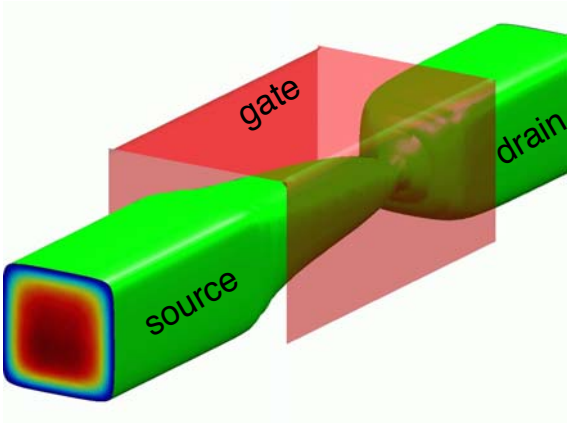

FIG. 2: Electron density isosurface (n=1.4 × 10^{19} cm^{-3}) computed for the SNWT with channel length equal to 15 nm, for a gate voltage V_{GS} = 0.5 V and a source-to-drain voltage V_{DS} =0.5 V.

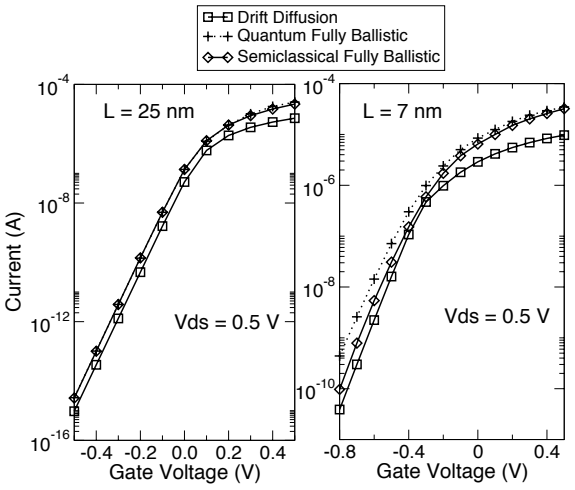

FIG. 3: Transfer characteristics computed for V_{DS} = 0.5 V, for the L = 25 nm and L = 7 nm devices.

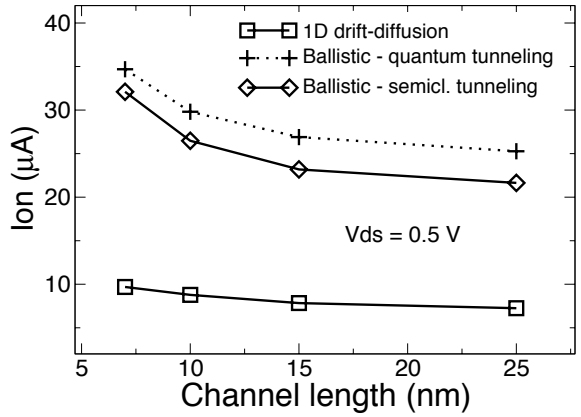

FIG. 4: I_{on} current as a function of the channel length

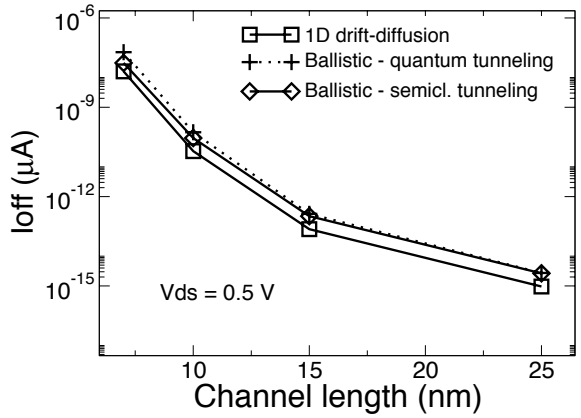

FIG. 5: I_{off} current as a function of the channel length

be avoided modifying eq. (4), inserting a Maxwell-Boltzmann like correcting factor

$$n = \sum_{i}^{M} |\psi_i|^2 n_{1D_i} \exp\left(\phi - \tilde{\phi}\right) \qquad (5)$$

III. RESULTS AND DISCUSSIONS

In Fig. 1 the simulated SNWT structure is shown. The oxide thickness is 1.5 nm, and the channel length L ranges from 7 to 25 nm. Degenerate statistics is considered in the wire. For simplicity, the gate is metallic.

In Fig. 2 the isosurface of the electron concentration for a device with channel length equal to 15 nm nanometer is shown : the gate and the source-to-drain voltages are equal to 0.5 V, i.e. the device is in the saturation regime, as confirmed by the constriction in correspondence of the drain.

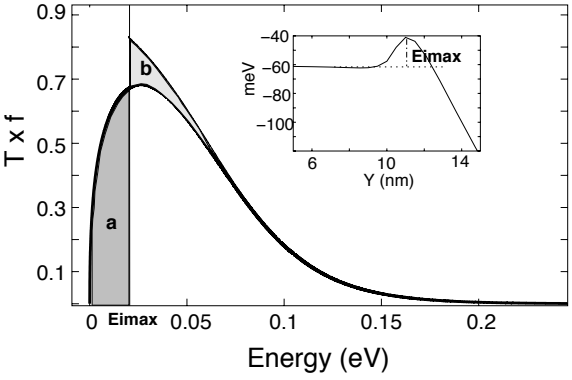

FIG. 6: Argument of integral in Equation (1). The upper curve is the argument in the semiclassical case, while the lower curve the argument in the quantum case. Tunneling current is larger than the semiclassical current, since the area **a** is larger than the area **b**.

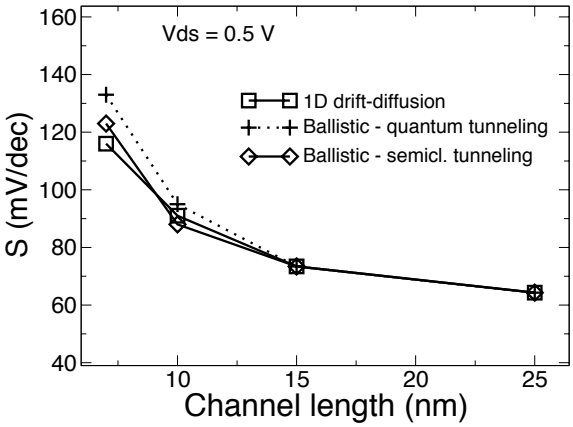

FIG. 7: Sub-threshold slope as a function of the channel length

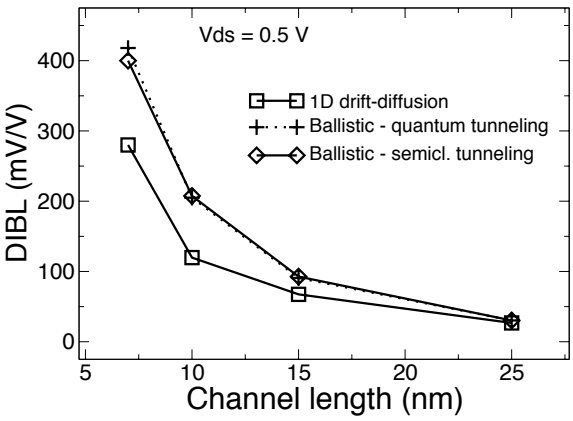

FIG. 8: Drain Induced Barrier Lowering as a function of the channel length

In Fig. 3 the transfer characteristics are plotted for

L=25 nm and L=7 nm, respectively, for a drain-to-source voltage V_{DS}=0.5 V. It is evident that for both devices the current in the ballistic case is much higher than in the drift-diffusion case. For a channel length of 7 nm source-to-drain tunneling is significant both in sub-threshold and in strong inversion conditions, while for L=25 nm tunneling is quantitatively relevant only in strong inversion. Such behavior is more clear if we consider I_{on} and I_{off} as a function of L , shown in Figs. 4 and 5, respectively. We have defined I_{off} as the current obtained for V_{DS} = 0.5 V and V_{GS} = - 0.5 V, and I_{on} as the current obtained for V_{DS} = 0.5 V and V_{GS} = 0.5 V. The dependence of I_{on} on L is rather small, in all transport regimes. Quantum tunneling gives a contribution only slightly dependent on L , and significant already for L=25 nm.

The reason can be understood considering that, for example, for L=25 nm the product of the transmission probability times the occupation factor has the energy dependence shown in Fig. 6, for semiclassical tunneling (thin line) and quantum tunneling (thick line).

The subband current is proportional to the area below the curve. Quantum tunneling adds a contribution that is proportional to the difference between the area **a** and the area **b**. The shape of the subband peak, shown in the inset, determines **a** and **b**, and depends essentially on the vertical electrostatics, and only marginally on L . Even for L=25 nm the barrier depth is only about 3 nm. On the other hand, I_{off} is affected by quantum tunneling only for L=10 nm, and is extremely sensitive to the channel length. Such dependence is mainly due to the degradation of the subthreshold slope S with decreasing length (shown in Fig. 7). Down to 15 nm, S is very good (<70 mV/dec).

For smaller L , S is degraded by charge sharing, but is still acceptable. Conversely, Drain Induced Barrier Lowering (DIBL) is much higher for ballistic than for drift-diffusion transport, as shown in Fig. 8. In the former case, current is essentially controlled by the subband peak, while in the latter, it is roughly dependent on the whole region between the source and the subband peak, that is farther from the drain.

IV. CONCLUSIONS

In conclusion, we have investigated the electrical properties of SNWTs with a detailed quantum simulation code, considering both drift-diffusion and ballistic transport, in order to evaluate the limiting cases for the performance of partially ballistic devices. SNWTs offer promising scaling perspectives down to 7 nm channel lengths, predicted at the end of the ITRS Roadmap. In addition, we have shown that the impact of quantum tunneling is significant also in strong inversion, and depends essentially on the vertical electrostatics rather than on L.

Acknowledgment

Support from the EU SINANO NoE (contract no. 506844) and from the MIUR-PRIN "Architectures and models for nanoMOSFETs" is gratefully acknowledged.

[1] International Technology Roadmap for Semiconductor 2003, Semiconductor Industry Association, S. Josè, USA (http://public.itrs.net)

[2] J.T. Park, and J.P. Colinge, *IEEE Trans. Elect. Dev.*, Vol. 49, pp.2222-2229, Dec. 2002.

[3] J.P. Colinge, J.T. Park, and C.A. Colinge, *Proc. International Conference on Microelectronics (MIEL 2002)*, 2002, pp. 109-113.

[4] T. Saito, T. Saraya, T. Inukai, H. Majimi, T. Nangumo, and Hiramoto. *IEICE Trans. Electron*, Vol. E85-C, No. 5, p.1073, 2002.

[5] B.Y., L. Chang, S. Ahmed, H. Wang, S. Bell, C.Y. Yang, C. Tabery, C. Ho, Q. Xiang, T.J. King, J. Bokor, C. Hu, M.R. Lin, and D. Kyser. *IEDM Tech. Dig.*, p. 107, 2001.

[6] A. Burenkov, and J. Lonenz, *ESSDERC '03*, 2003, pp. 135-138.

[7] B. S. Doyle, S. Datta, M. Doczy, S/ Hareland, B.J. Kavalieros, T. Linton, A. Murthy, R. Rios, and R. Chau, *IEEE Trans. Elect. Dev.*, Vol. 24, pp. 263-265, Apr. 2003.

[8] H.Majima, Y. Saito, and T. Hiramoto, *IEDM Tech. Dig.*, p. 733, 2001.

[9] J. Wang, E. Polizzi, and M. Lundstrom *IEDM Tech. Dig.*, 2003, pp. 29.5.1-29.5.4.

[10] A. Lochtefeld, and D.A. Antoniadis, *IEEE Electron Device Lett.*, Vol. 22, pp.95-97, Feb. 2001.

[11] J. C. Inkson, *Many body theory of solids- an introduction*, New York: Plenum, 1984, pp.209-231.

[12] A. Trellakis, A.T. Galick, A. Pacelli, and U. Ravaioli, *J. Appl. Phys*, Vol. 81, pp. 7880-7884, Mar. 1997.

[13] S. Datta, *Electronic Transport in Mesoscopic Systems*, Cambridge UK : Cambridge University Press, 1998, pp. 29-31.

[14] G. Fiori, G.Iannaccone, *Applied Physics Letters*, pp. 3672-3674, Nov. 2002.

[15] D. L. Scharfetter, and D. L. Gummel, *IEEE Trans. Elect. Dev.*, vol. ED-16, pp.64-77, 1969.

[16] D.M. Caughey, R.E. Thomas, *IEEE Proc.*, Vol. 55, pp.2192-2193, 1967.

[17] D.B.M. Klaassen, *Solid-State Electronics*, Vol. 35, pp.953-959, Dec. 1992.